

Numerical Investigations of Mixing Performance in Split and Recombine Micromixer



Ekta Tripathi, Promod Kumar Patowari, and Sukumar Pati

1 Introduction

In this modern era, quick and uniform mixing is essential in various microfluidic areas such as LOC (lab on the chip) devices, μ -total analysis systems, biological and chemical synthesis [1–4]. In microfluidic devices, the mixing of fluids depends on molecular diffusion that reduces the mixing time of fluids due to laminar characteristics of flow. Various active and passive micromixers have been designed by several researchers with the purpose of increasing the mixing performance. Active micromixers require an external drive to generate energy for stirring the fluids to achieve fast mixing [1, 3–5], whereas in passive micromixers, mixing can be upgraded by designing or altering the geometries and shapes of the micromixers.

Several numerical and experimental studies have been performed in various micromixers as these micromixers are easy to fabricate by soft lithography techniques [6–8]. Mixing characteristics are analyzed in various micromixers by implementing various design concepts such as multiwave, square wave, zigzag, C-type, spiral contours. Channel walls are modified by ribs and grooves, placing the obstacles in the micromixers to disturb the flow are also introduced in order to enhance the mixing [9–14]. Sudarsan and Ugaz [15] considered planar split and recombine (S-R) and asymmetric serpentine micromixers to examine the mixing and flow characteristics of fluids. Both micromixers are found efficient in short downstream length. Hossain and Kim [16] analyzed mixing performance of water and ethyl alcohol in 3D serpentine S-R micromixer having special type segments (OH segments) and

E. Tripathi (✉) · P. K. Patowari · S. Pati
Mechanical Engineering Department, NIT Silchar, Silchar, Assam, India
e-mail: ekta_rs@mech.nits.ac.in

P. K. Patowari
e-mail: ppatowari@mech.nits.ac.in

S. Pati
e-mail: sukumar@mech.nits.ac.in

reported that SAR micromixer is more efficient than serpentine one. Hossain et al. [17] proposed an unbalanced three split rhombic sub-channel-based micromixer for studying the mixing and flow characteristics for $30 \leq Re \leq 80$ and reported high mixing efficiency. Raza et al. [18] also used the concept of S-R in 3D serpentine micromixers with crossing channels by generating saddle type flow arrangement, which increases the chaotic advection even at low Reynolds numbers.

Numerous studies have been performed in S-R micromixers by various researchers. From the literature, it has been observed that nominal work has been done on different configurations of S-R geometry. In this paper, various types of S-R micromixers are designed by changing the shape of wall boundaries and inside grooves to examine the effect of shapes of S-R micromixers on the mixing performance of fluids in the micromixers. Mixing characteristics and pressure drop of mixing fluids are compared in these micromixers for low ranges of Re .

2 Problem Statement

First, a split and recombine (S-R) micromixer is designed having a square inner groove and square wall boundaries as shown in Fig. 1a, and the geometry is abbreviated as SiSo. Two fluids enter the micromixers in two opposite sides. The main width of the micromixers is 0.1 mm. After traveling 0.5 mm in the main mixing chamber, fluids split and again recombine in the square grooves-based chamber. Both width and depth of the outer square grooves are 0.2 mm whereas the width and depth of inner grooves are 0.1 mm. Eight such chambers are designed at 0.1 mm distance. The exit length is 0.5 mm. Figure 1b represents the second S-R geometry (TiTo) with triangular inner grooves and triangular outer wall boundaries. Figure 1c represents the S-R geometry (abbreviated as SiTo) in which the inner grooves are square and outer wall boundaries are triangular. The fourth micromixer (abbreviated as TiSo) is

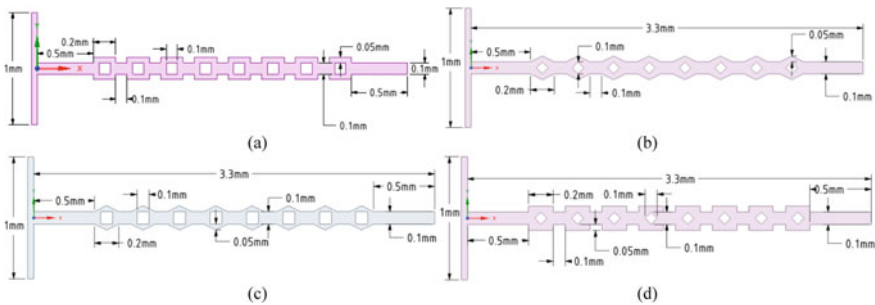


Fig. 1 Schematics of S-R micromixers. (a) Both outer boundary and inner grooves of square shape (SiSo), (b) Both outer boundary and inner grooves of triangular shape (TiTo), (c) Outer boundary of triangular and inner of square shape (SiTo), (d) Outer boundary of square shape and inner of triangular shape (TiSo)

designed with triangular inner grooves and square outer wall boundaries. The sizes of all these grooves are taken exactly the same.

3 Mathematical Formulation

The velocity and pressure fields for a two-dimensional, steady-state, laminar, incompressible, isothermal, and single-phase flow in the micromixers are acquired using equations of continuity and Navier stokes for Newtonian fluids.

$$\nabla \cdot (\vec{U}) = 0 \quad (1)$$

$$(\vec{U} \cdot \nabla) \vec{U} = -\frac{1}{\rho} \nabla P + \nu (\nabla^2 \vec{U}) \quad (2)$$

Here, \vec{U} is the velocity vector, ρ is the fluid density (kg m^{-3}), P is pressure (Pa), ν is kinetic viscosity of fluids (ms^{-2}).

The concentration field is obtained by solving the species transport equation as follows:

$$(\vec{U} \cdot \nabla) \mathcal{C} = \alpha (\nabla^2 \mathcal{C}) \quad (3)$$

Here, \mathcal{C} is the concentration of the species (mol-m^{-3}) and α is the coefficient of diffusion ($\text{m}^2 \text{s}^{-1}$).

Uniform inlet velocity and atmospheric pressure at the outlet and 0 slip boundary conditions at the walls are considered.

The mixing quality is quantified by the mixing index. It is determined by calculating the standard deviation of species in the perpendicular plane to the fluid flow. The standard deviation of the mass fraction of the fluid in any mixture at a cross-sectional plane is considered as

$$SD = \sqrt{\frac{\sum_{j=1}^r (C_j - \overline{C_k})^2}{r}} \quad (4)$$

where SD is standard deviation of mass fraction in the particular cross-sectional area, r is overall number of sampling points, C_j is the mass fraction at sampling point j , and $\overline{C_k}$ is average mixing mass fraction. After calculating the SD , the mixing index (MI) is calculated as

$$MI = 1 - \frac{SD}{SD_{\max}} \quad (5)$$

where SD_{max} is the standard deviation of the completely unmixed state. It may be noted that the range of MI is 0 for fully unmixed fluids to 1 for fully mixed fluids.

4 Numerical Simulations

Numerical simulations are performed in Ansys-18.1 (Fluent). Water and water-dye solution are used as fluids for mixing. The viscosity of water is 0.9×10^{-3} Pa-s and density is 1000 kg/m^3 . The diffusion coefficient for water and water-dye solution is taken as $1.2 \times 10^{-9} \text{ m}^2/\text{s}$. The SIMPLER algorithm is applied for the pressure and velocity compounding. Second order upwind scheme is selected for discretization of the advection terms. For convergence, root mean square (RMS) residual is set as 10^{-5} .

A detailed grid independency test is carried out to select the grid for actual simulation in order to minimize the computational cost and time without compromising the accuracy. A graph has been plotted (Fig. 2) between pressure drop and mixing index with the total number of elements for each micromixer configuration. From the graph, it is obvious that pressure drop and mixing index are constant after a certain value of elements. From the graph plot, grids with 326,903, 195,108, 328,959, and

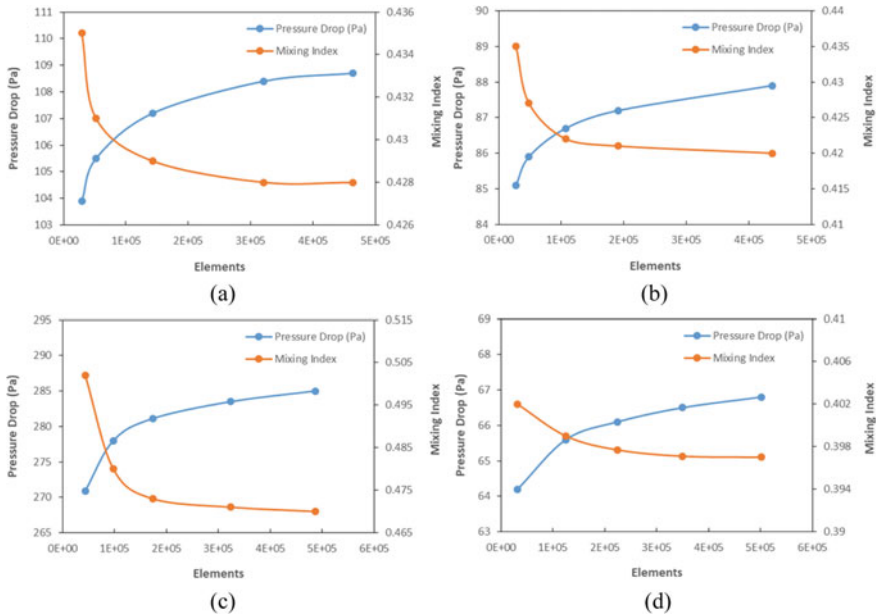


Fig. 2 Variation of pressure drop (on the primary vertical axis) and mixing index (on the secondary vertical axis) with grid elements (on the horizontal axis) for grid-independent test for micromixer **a** SiSo, **b** TiTo, **c** SiTo and **d** TiSo

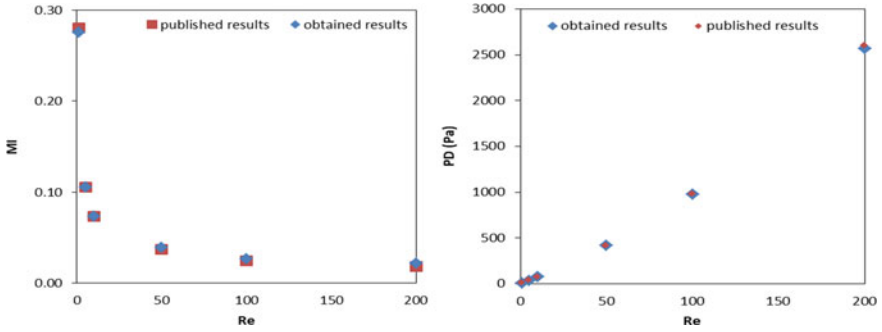


Fig. 3 Validation of (a) MI (mixing index) and (b) pressure drop with Re with the results reported in [19]

354,679 number of elements are selected for SiSo, TiTo, SiTo, and TiSo micromixers, respectively, for further calculations.

To ensure the accuracy of adopted numerical methodology in the present work, the solver is validated by comparing the mixing index and pressure drop with the results reported in [19] for a T-shape micromixer as presented in Fig. 3. As shown in Fig. 3a, b obtained and published results are compared, and it shows that both results are approximately the same, which proves the authenticity of the simulation work.

5 Result and Discussion

The focus of the work is to analyze the effect of groove shapes on the mixing characteristics of fluids and pressure-drop in the split and recombine (S-R) microchannels

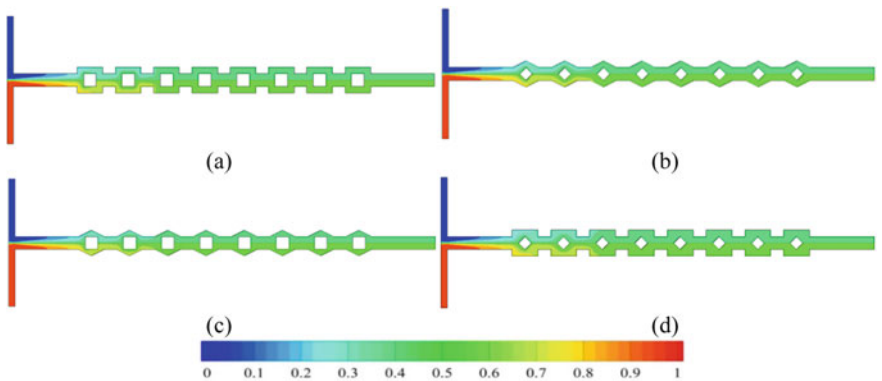


Fig. 4 Concentration contours of water at Re = 0.1 in (a) SiSo, (b) TiTo, (c) SiTo and (d) TiSo

for Reynolds number in the range of $0.1 \leq Re \leq 1$. Figure 4 represents the concentration contours of fluids at $Re = 0.1$ in each micromixer. Two fluids enter into the microchannel. For ideal mixing, the concentration plot should be uniform at the outlet of the channel throughout the cross-section. It is seen that at $Re = 0.1$, from chamber 3 onwards, almost green color appears, indicating the proper mixing in the channel. It is because of the low velocities of fluids at $Re = 0.1$, mixing or diffusion time to mix the fluids is more. Figure 5 represents the concentration contours of fluids at $Re = 0.6$ in all the micromixers. Here, mixing is diminished than that of $Re = 0.1$ as when Re is increased to 0.6, the significant difference in the concentration can be seen in each micromixer. For $Re = 1$, the difference in the concentration increases more, as shown in Fig. 6. It indicates the lower mixing efficiency of the fluids at a higher Reynolds number. The trends of concentration contours in all the micromixers are almost the same with Re .

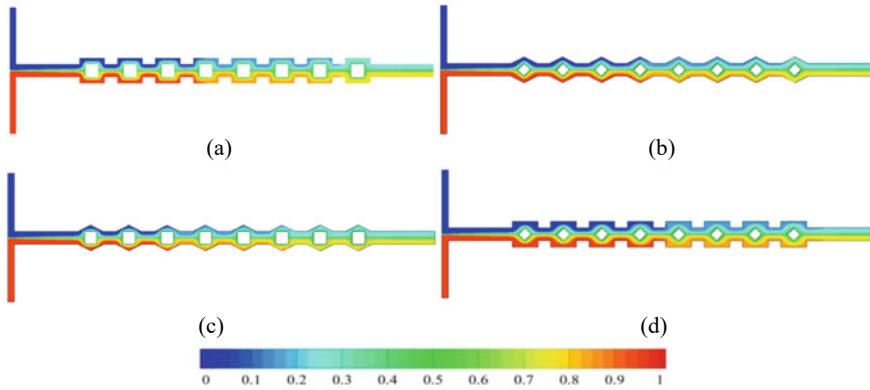


Fig. 5 Concentration contours of fluids at $Re = 0.6$ in (a) SiSo, (b) TiTo, (c) SiTo and (d) TiSo

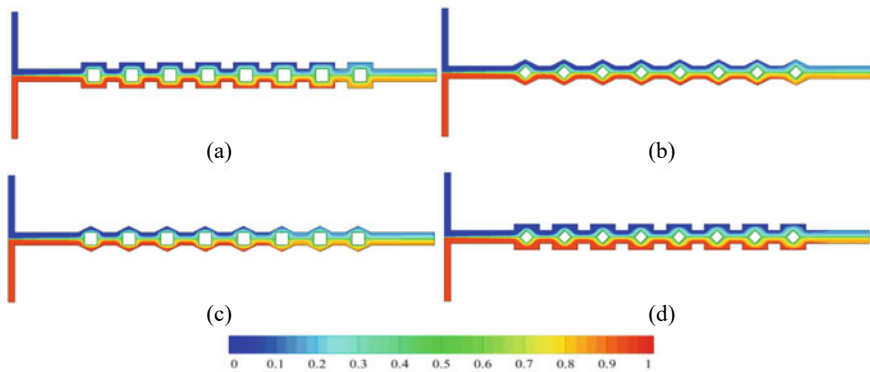


Fig. 6 Concentration contours of fluids at $Re = 1$ in (a) SiSo, (b) TiTo, (c) SiTo and (d) TiSo

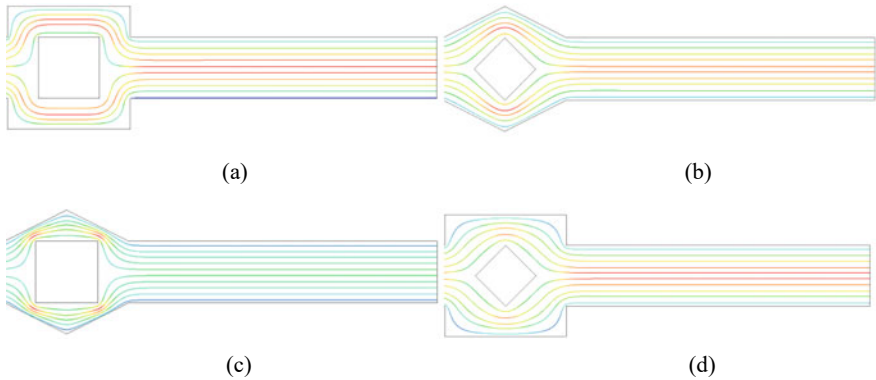


Fig. 7 Streamlines distribution in micromixers at $Re = 1$ in (a) SiSo, (b) TiTo, (c) SiTo and (d) TiSo micromixers

For the more comprehensive detail, streamlines distribution near the outlet in each micromixer is shown in Fig. 7 at $Re = 1$. Streamlines distribution are almost identical in SiSo and TiTo, as represented in Fig. 7a, b. It is clearly depicted that streamlines in SiTo (Fig. 7c) are closely packed near to the grooves, whereas in TiSo as shown in Fig. 7d, these streamlines maintain an almost equal distance from each other. This representation of streamlines in the microchannel shows the cause of different mixing indexes in the microchannel. Closely packed streamlines result in higher mixing than that of others.

The mixing index for different micromixers is compared at various Reynolds numbers in Fig. 8a. At $Re = 0.1$, the value of MI is the maximum, and it is almost the same for all the geometry. The change in the flow path has almost no influence because of the sufficient time for diffusion. It is observed that MI decreases with an increase in Re . It is due to a reduction in the diffusion mixing time with Re , and the homogeneity is completely diffusion controlled. The value of the mixing index is the highest in SiTo, whereas in TiSo, it is the lowest for $Re \geq 0.2$. The values

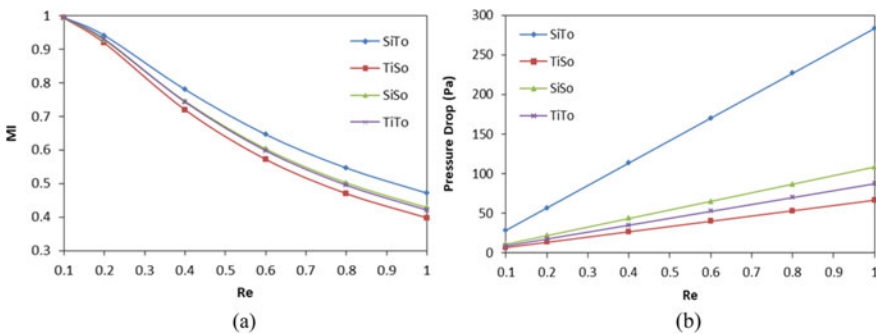


Fig. 8 Variation of (a) mixing index with Re and (b) pressure drop with Re for different micromixers

of the mixing index are almost the same for SiSo and TiTo micromixers, even for $Re \geq 0.2$. The flow passages of two fluids in the micromixers are divided and again recombined and importantly, the shape of the grooves modulates the same. In SiTo, more fluids come in contact because of the confined passage, and the fluids mixing takes place as it comes in contact more rapidly. That is why the mixing index in SiTo is more than that of other micromixers. On the other hand, in TiSo, fluids do not have enough contact to diffuse into each other, leading to the lower mixing index.

It is also vital to analyze the pressure drop in each micromixer. A pressure drop indicates the required driving force for fluid flow inside the micromixers. The pressure drop and Re graph for various micromixer geometry are demonstrated in Fig. 8b. From Fig. 8b, it is clear that the pressure drop increases with an increase in Re . The high value of Re means an increase in velocity that leads to the high-pressure drop irrespective of any geometrical parameters. On comparing, the pressure drop in different micromixer geometry for any values of Re , the pressure drop is the maximum in SiTo due to the more losses incurred in the flow as shown by the curvature of the streamlines (Fig. 7c). The difference of pressure drop between different configurations increases with Reynolds number.

6 Conclusion

In this present paper, pressure drop and flow characteristics are analyzed for two-dimensional, Newtonian, incompressible, steady flows in various split and recombine (S-R) micromixers. Four different configurations of micromixers are designed by considering the different shapes of grooves. The mixing characteristics and pressure drop for Re ranges from 0.1 to 1 are analyzed in the designed micromixers. The main outcomes of this research are concluded as:

- The mixing index reduces at higher Reynolds number in all the micromixers. At $Re = 0.1$, the mixing is the maximum, and the value is almost the same for all the geometry.
- The pressure drop increases with the Reynolds number for all the micromixers. Maximum pressure drop of 283 Pa at $Re = 1$ and minimum of 28 Pa at $Re = 0.1$ is observed in SiTo, whereas maximum pressure drop of 66 Pa at $Re = 1$ and minimum of 6.7 Pa at $Re = 0.1$ are observed in TiSo.
- The mixing quality is the highest in SiTo, whereas in TiSo, it is the lowest for $Re \geq 0.2$. The mixing index values are approximately equal for SiSo and TiTo micromixers, even at $Re \geq 0.2$.
- Even though SiTo shows highest mixing index but due to the high-pressure drop, it is not recommended whereas TiTo shows second-best mixing index and relatively much lower pressure drop in the channel than that of SiTo. Thus, TiTo could be used for industrial mixing purposes.

References

1. Nguyen N (2011) *Micromixers: fundamentals, design and fabrication*. Elsevier Science, Netherlands
2. Ingham CJ, van Hylckama Vlieg JE (2008) MEMS and the microbe. *Lab Chip* 8(10):1604–1616
3. Hessel V, Löwe H, Schönfeld F (2005) Micromixers—a review on passive and active mixing principles. *Chem Eng Sci* 60(8–9):2479–2501
4. Nguyen NT, Wu Z (2005) Micromixers—a review. *J Micromech Microeng* 15:R1
5. Mehta SK, Pati S, Mondal PK (2021). Numerical study of the vortex induced electroosmotic mixing of non-Newtonian biofluids in a non-uniformly charged wavy microchannel: effect of finite ion size. *Electrophoresis*. <https://doi.org/10.1002/elps.202000225>
6. Tripathi E, Patowari PK, Pati S (2019) Fabrication of spiral micromixer using mold machined by CO₂ assisted laser machine. In: Paper presented at 11th international conference on precision, meso, micro and nano engineering (COPEN 11). IIT Indore, 12–14 Dec 2019
7. Mondal B, Pati S, Patowari PK (2020) Fabrication of wavy micromixer using soft lithography technique. *Mater Today Proc* 26:1271–1278
8. Mondal B, Pati S, Patowari PK (2021) Serpentine square wave microchannel fabrication with WEDM and soft lithography. *Mater Today Proc*. <https://doi.org/10.1016/j.matpr.2021.03.519>
9. Mondal B, Mehta SK, Patowari PK, Pati S (2019) Numerical study of mixing in wavy micromixers: comparison between raccoon and serpentine mixer. *Chem Eng Process Process Intensifi* 136:44–61
10. Mondal B, Pati S, Patowari PK (2020) Numerical analysis of mixing performance in microchannel with different ratio of outlet to inlet width. In: *Techno-societal 2018*. Springer, Cham, pp 257–266
11. Tripathi E, Patowari PK (2020) Design and computational analysis of spiral microchannel for mixing of fluids. In: *Techno-societal 2018*. Springer, Cham, pp 305–313
12. Tripathi E, Patowari PK, Pati S (2021) Comparative assessment of mixing characteristics and pressure drop in spiral and serpentine micromixers. *Chem Eng Process Process Intensifi* 162:108335
13. Mondal B, Pati S, Patowari PK (2019) Analysis of mixing performances in microchannel with obstacles of different aspect ratios. *Proc Inst Mech Eng Part E J Process Mech Eng* 233(5):1045–1051
14. Mondal B, Pati S, Patowari PK (2020) Influence of confluence angle between inlets on the mixing performance of micro-mixer with obstacles. In: *Techno-societal 2018*. Springer, Cham, pp 275–283
15. Sudarsan AP, Ugaz VM (2006) Multivortexmicromixing. *Proc Natl Acad Sci* 103(19):7228–7233
16. Hossain S, Kim KY (2015) Mixing analysis in a three-dimensional serpentine split-and-recombine micromixer. *Chem Eng Res Des* 100:95–103
17. Hossain S, Kim KY (2014) Mixing analysis of passive micromixer with unbalanced three-split rhombic sub-channels. *Micromachines* 5(4):913–928
18. Raza W, Hossain S, Kim KY (2018) Effective mixing in a short serpentine split-and-recombination micromixer. *Sens Actuators B Chem* 258:381–392
19. Solehati N, Bae J, Sasmito AP (2014) Numerical investigation of mixing performance in microchannel T-junction with wavy structure. *Comput Fluids* 96:10–19